Received: 15 March 2021 | Revised: 31 August 2021 | Accepted: 1 September 2021

DOI: 10.1002/bit.27938

ARTICLE

BIOTECHNOLOGY AND BIOENGINEERING WILEY

Pseudomonas putida KT2440 endures temporary oxygen limitations

Philipp Demling[1] | Andreas Ankenbauer[2] | Bianca Klein[3] | Stephan Noack[3] | Till Tiso[1] | Ralf Takors[2] | Lars M. Blank[1]

[1]Institute of Applied Microbiology (iAMB), Aachen Biology and Biotechnology (ABBt), RWTH Aachen University, Aachen, Germany

[2]Institute of Biochemical Engineering, University of Stuttgart, Stuttgart, Germany

[3]Institute of Bio- and Geosciences (IBG-1): Biotechnology, Forschungszentrum Jülich GmbH, Jülich, Germany

Correspondence
Till Tiso and Lars M. Blank, Institute of Applied Microbiology, Aachen Biology and Biotechnology, RWTH Aachen University, Worringer Weg 1, 52074 Aachen, Germany.
Email: till.tiso@rwth-aachen.de and lars.blank@rwth-aachen.de

Funding information
Deutsche Forschungsgemeinschaft, Grant/Award Number: FSC 2186; H2020 Industrial Leadership, Grant/Award Number: 635536; Bundesministerium für Bildung und Forschung, Grant/Award Number: 031B0350B

Abstract

The obligate aerobic nature of *Pseudomonas putida*, one of the most prominent whole-cell biocatalysts emerging for industrial bioprocesses, questions its ability to be cultivated in large-scale bioreactors, which exhibit zones of low dissolved oxygen tension. *P. putida* KT2440 was repeatedly subjected to temporary oxygen limitations in scale-down approaches to assess the effect on growth and an exemplary production of rhamnolipids. At those conditions, the growth and production of *P. putida* KT2440 were decelerated compared to well-aerated reference cultivations, but remarkably, final biomass and rhamnolipid titers were similar. The robust growth behavior was confirmed across different cultivation systems, media compositions, and laboratories, even when *P. putida* KT2440 was repeatedly exposed to dual carbon and oxygen starvation. Quantification of the nucleotides ATP, ADP, and AMP revealed a decrease of intracellular ATP concentrations with increasing duration of oxygen starvation, which can, however, be restored when re-supplied with oxygen. Only small changes in the proteome were detected when cells encountered oscillations in dissolved oxygen tensions. Concluding, *P. putida* KT2440 appears to be able to cope with repeated oxygen limitations as they occur in large-scale bioreactors, affirming its outstanding suitability as a whole-cell biocatalyst for industrial-scale bioprocesses.

KEYWORDS
metabolic engineering, plug flow reactor, *Pseudomonas putida*, rhamnolipids, scale-down, temporary oxygen limitation

1 | INTRODUCTION

Recently, *Pseudomonas putida* has emerged as a promising host for industrial bioprocesses (Ankenbauer et al., 2020; Nikel & de Lorenzo, 2018; Tiso et al., 2014; Weimer et al., 2020). Its versatile carbon metabolism allows the usage of different carbon sources (Blank et al., 2020; Hintermayer & Weuster-Botz, 2017; Weimer et al., 2020), potentially contributing to valorize waste streams for the production of value-added compounds in the scope of an envisioned circular bioeconomy. Prominent examples are the production of rhamnolipids from xylose (Bator, Wittgens, et al., 2020) and the upcycling of plastic waste (Tiso et al., 2021) using recombinant *P. putida* as a whole-cell

biocatalyst. Further, *P. putida* has been shown to flexibly respond to several environmental perturbations like oxidative stress (Nikel et al., 2020) and, most prominently, tolerating high concentrations of toxic substances such as organic solvents (Nikel & de Lorenzo, 2014; Ramos et al., 2015; Simon et al., 2015). This ability allows the application of an organic solvent phase, for example, in process intensification by in situ extractions (Demling et al., 2020; Wierckx et al., 2005).

P. putida KT2440 is considered the most suitable candidate among pseudomonads for industrial applications due to its host-vector (HV) system safety level 1 status (Kampers, Volkers, et al., 2019), facilitating accreditations for production processes. Further, the ability of *P. putida* KT2440 to withstand industrial-scale stress conditions in terms of fluctuations in carbon availability has recently been demonstrated (Ankenbauer et al., 2020), indicating its potential to cope with nutrient gradients and local limitations due to nonideal mixing, typically occurring in large-scale fermenters (Enfors et al., 2001; Lara et al., 2006). In this regard, recent computational fluid dynamic simulations predict mean residence times up to 76 s for bacterial cells in low glucose or low oxygen regimes inside a 300 L pilot-scale bioreactor (Kuschel & Takors, 2020). Therefore, zones within the fermenter exhibiting low oxygen concentrations pose a potential drawback to establish industrial-scale fermentations, particularly with obligate aerobic organisms such as *P. putida* KT2440. Further, in the scope of recent advances in bioreactor design, specialized apparatuses have emerged, which exhibit intentionally non-aerated compartments, leading to reactor zones with low oxygen availability (Bednarz et al., 2017; Weber et al., 2019). As inhomogeneous mixing hardly occurs in laboratory-scale fermentations, specialized scale-down reactors have been developed to intentionally induce ambient perturbations (Enfors et al., 2001; Neubauer & Junne, 2010; Neubauer et al., 1995). Considering oxygen, many studies have focused on mimicking gradients and transitions using model organisms (Nadal-Rey et al., 2020; Olughu et al., 2019) like *Escherichia coli* (Soini et al., 2008) or other industrially relevant microorganisms like *Corynebacterium glutamicum* (Käß et al., 2014; Lange et al., 2018; Limberg et al., 2017) in scale-down reactors. However, the yeasts *Pichia pastoris* (Lorantfy et al., 2013) and *Yarrowia lipolytica* (Bellou et al., 2014; Kar et al., 2012; Timoumi et al., 2017) have been the only studied microorganisms regarded as being obligate aerobic.

Several efforts have been made to engineer *P. putida* KT2440 to be capable of either anaerobic fermentation or anaerobic respiration (Nikel & de Lorenzo, 2013; Sohn et al., 2010; Steen et al., 2013). While survival of the engineered strains was successfully demonstrated, growth or the production of value-added compounds could not be sustained. However, with oxygen levels below detection limit, an isobutanol producing *P. putida* derivative revealed minimal metabolic activity for several hours (Ankenbauer et al., 2021; Nitschel et al., 2020). Further, in the absence of oxygen, bioelectrochemical systems (BES) could be employed to enable the synthesis of different products (Lai et al., 2016; Schmitz et al., 2015; Yu et al., 2018). Recently, a proof of concept for rhamnolipid production in an oxygen-limited BES was reported (Askitosari et al., 2020). Applying in silico approaches, Kampers, van Heck, et al. (2019) identified several limitations for establishing anaerobic metabolism and a derived strategy for rational strain engineering enabled *P. putida* KT2440 to grow under micro-oxic conditions. However, for a fully anaerobic metabolism, further extensive strain engineering has been predicted (Kampers et al., 2021).

As oxygen concentrations in industrial-scale fermenters are typically fluctuating and subject to gradients, we propose that introducing a fully anaerobic metabolism into *P. putida* KT2440 is not stringently required, but rather its ability to cope with altering conditions needs to be evaluated and potentially enhanced. Thus, in this study, we assess the ability of *P. putida* KT2440 to endure temporary oxygen limitations. Different scale-down approaches, ranging from disturbed cultivations in microtiter plates (MTPs) to cultivations in stirred-tank reactors (STRs) and a defined compartmented reactor, are used to mimic industrial-scale reactor inhomogeneities in terms of oxygen availability to evaluate its effect on the growth of *P. putida* KT2440. Here, cultivations in different laboratories and operational conditions were performed to assess the robustness of *P. putida* KT2440 in varying settings. Additionally, the influence of repeated oxygen limitations on the production of secondary metabolites, here for the example of rhamnolipids, by a recombinant *P. putida* KT2440 is assessed.

2 | MATERIALS AND METHODS

2.1 | Strains, products, and media

P. putida KT2440 (DSMZ: 6125; Bagdasarian et al., 1981; Nakazawa, 2002) was used for cultivations performed to assess the growth behavior at temporary oxygen starvation. A recombinant *P. putida* KT2440 strain constitutively producing mono-rhamnolipids (mono-RLs) and their precursors 3-(hydroxyalkanoyloxy)alkanoic acids (HAAs), collectively referred to as RLs hereafter, was cultivated. The strain was previously engineered by integrating *rhlA* and *rhlB* from *Pseudomonas aeruginosa* into the genome of *P. putida* KT2440 at the *att*Tn7 site. The resulting strain *P. putida* KT2440 *att*Tn7::*Pffg-rhlAB* is further referred to as *P. putida* KT2440 SK4 (Tiso et al., 2020).

For secondary seed cultivations and MTP cultivations, mineral salts medium modified from Hartmans et al. (1989) was used (10 g L^{-1} glucose, 11.64 g L^{-1} K_2HPO_4, 4.89 g L^{-1} NaH_2PO_4, 2 g L^{-1} $(NH_4)_2SO_4$, 0.1 g L^{-1} $MgCl_2{\cdot}6H_2O$, 10 mg L^{-1} EDTA, 2 mg L^{-1} $ZnSO_4{\cdot}7H_2O$, 1 mg L^{-1} $CaCl_2{\cdot}2H_2O$, 5 mg L^{-1} $FeSO_4{\cdot}7H_2O$, 0.2 mg L^{-1} $Na_2MoO_4{\cdot}2H_2O$, 0.2 mg L^{-1} $CuSO_4{\cdot}5H_2O$, 0.4 mg L^{-1} $CoCl_2{\cdot}6H_2O$, and 1 mg L^{-1} $MnCl_2{\cdot}2\ H_2O$). The mineral salts medium was highly buffered to counteract the pH-decrease due to the production of gluconate and 2-ketogluconate.

For continuous cultivations in the STR-PFR setup, M12 mineral salts medium (Vallon et al., 2013) was used (17 g L^{-1} glucose, 2.2 g L^{-1} $(NH_4)_2SO_4$, 0.4 g L^{-1} $MgSO_4{\cdot}7H_2O$, 0.04 g L^{-1} $CaCl_2{\cdot}2H_2O$, 0.02 g L^{-1} NaCl, 2 g L^{-1} KH_2PO_4, 2 mg L^{-1} $ZnSO_4{\cdot}7H_2O$, 1 mg L^{-1} $MnCl_2{\cdot}4H_2O$, 15 mg L^{-1} $Na_3C_6H_5O_7{\cdot}2H_2O$, 1 mg L^{-1} $CuSO_4{\cdot}5H_2O$, 0.02 mg L^{-1} $NiCl_2{\cdot}6\ H_2O$, 0.03 mg L^{-1} $Na_2MoO_4{\cdot}2H_2O$, 0.3 mg L^{-1} H_3BO_3, and

10 mg L^{-1} $FeSO_4 \cdot 7H_2O$). A different medium compared to all other cultivations was used as the STR-PFR cultivations were performed in a different laboratory and the phenotype of *P. putida* KT2440 was to be evaluated in different operational settings.

2.2 | Strain propagation

For MTP and STR batch cultivations, cryopreserved *P. putida* KT2440 or *P. putida* KT2440 SK4 was streaked onto agar plates and incubated at 30°C for 24 h. Single colonies were used to inoculate 5 ml LB medium incubated at 30°C and 300 rpm in an orbital shaker (shaking diameter: 50 mm) for initial liquid seed cultures. Cells were transferred to a second seed culture at mid-exponential growth phase, consisting of 50 ml Hartmans mineral salts medium. The second seed culture was incubated at the same conditions as stated above and harvested for transfer into main cultures during mid-exponential growth. The initial seed train for the continuous STR-PFR cultivations was performed as described in Ankenbauer et al. (2020).

2.3 | Microtiter plate cultivations

MTP cultivations were performed in Round Well Plates (MTP-R48-B, m2p-labs; sealing: Breathseal Sealer, Greiner Bio-One) and were controlled by the BioLector I (m2p-labs). The filling volume of the wells was set to 1 ml Hartmans mineral salts medium, inoculated with wild-type *P. putida* KT2440 at an initial optical density of 0.05. The cultivation temperature was kept constant at 30°C, and humidity control was activated to limit evaporation. The oxygen transfer capacity (OTR_{max}) is dependent on the shaking frequency (Kensy et al., 2005). Therefore, to achieve temporary but repetitive low dissolved oxygen tensions (DOTs), a profile oscillating between 1200 rpm and 200 rpm for specific time intervals was established by developing a script implemented in the respective backend setups of each run (Figure 1a). According to the equation published by Lattermann et al. (2014) to estimate the OTR_{max} at different cultivation conditions, approximate OTR_{max} of 1.2 and 60.0 mmol L^{-1} h^{-1} have been calculated for low and high shaking frequencies, respectively, thereby validating intended oscillations. Time intervals of high and low shaking frequencies were identical within one cultivation, that is, the duration of vigorously shaking was equal to the duration of restricted shaking. Time intervals of 2 min, 4 min, and 6 min were compared to a control cultivation constantly shaking at 1200 rpm. Measurement intervals were synchronized with shaking intervals to record the backscatter signal (which correlates to biomass content) at a shaking frequency of 1200 rpm. Thereby, an erroneous signal caused by sedimented cells was avoided. Cultivations were performed in five biological replicates.

2.4 | Cultivations in stirred-tank reactors

Batch cultivations were performed in 3 L stirred-tank bioreactors fully controlled by BioFlo120 units and DASware Control Software 5.5.0 (all Eppendorf AG). The working volume was set to 2 L Hartmans minimal salts medium, which was inoculated to an initial optical density of 0.2 using the second seed culture. The buffer concentration was reduced threefold compared to the medium composition stated above due to active pH control. The pH initially set to a value of 7 was monitored with online pH probes (phferm, Hamilton Company) and kept constant by the automated addition of 4 M H_2SO_4 and 4 M KOH. The temperature was set to 30°C, and the DOT was monitored with invasive probes (VisiFerm, Hamilton Company). Agitation and aeration were periodically altered between low (25 rpm, 0 vvm) and high (800 rpm, 1 vvm) setpoints to induce an oscillating DOT throughout the cultivations (Figure 1b). Intervals of high and low DOT were set to equal durations of 2 min or 4 min. Control cultivations were aerated and agitated constantly at high setpoints. Oxygen and carbon dioxide concentrations in the exhaust gas

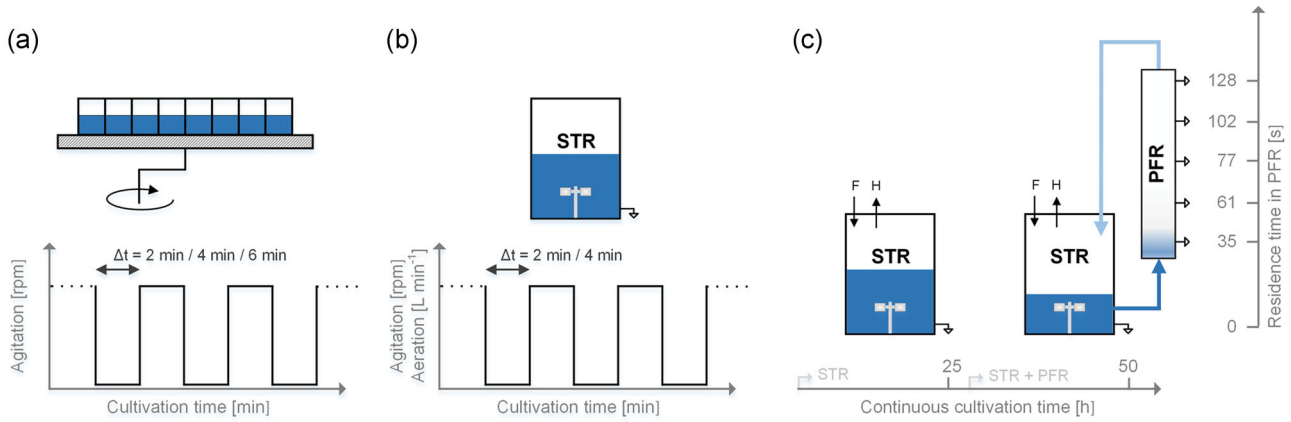

FIGURE 1 Schematic illustrations of different scale-down cultivation setups to mimic large-scale inhomogeneities in lab-scale. (a) MTP cultivations with oscillating shaking intervals. (b) STR cultivations with oscillating agitation and aeration. (c) An STR operated as glucose-limited chemostat with continuous medium feed [F] and harvest [H] served as reference conditions after reaching steady-state after five residence times. By connecting the PFR with the STR, dual substrate starvation by glucose and oxygen was applied. The STR and the five ports of the PFR were sampled simultaneously after further five residence times. MTP, microtiter plate; STR, stirred-tank reactor; PFR, plug flow reactor

were measured by BlueInOne Ferm Gas analyzers and monitored with BlueVis (both BlueSens GmbH).

Cultivations for assessing the influence of oscillating DOT on rhamnolipid production by *P. putida* KT2440 SK4 were performed at slightly modified conditions. To avoid foaming, 250 ml ethyl decanoate was added to the bioreactor for an in situ extraction of rhamnolipids. The pH was set to 6 to increase the partition coefficient and thus enhance the extraction efficiency, which has been described previously (Demling et al., 2020). The oscillating interval was set to 2 min. All STR cultivations were performed as biological duplicates.

2.5 | STR-PFR cultivation

First, steady-state growth was installed by operating a glucose-limited chemostat with a dilution rate of 0.2 h^{-1} in the STR. The scale-down setup was identical to Ankenbauer et al. (2020). The DOT was controlled at 5%, pH at 6.9, and temperature at 30°C. The culture was sampled after five residence times (≥25 h) in the STR to monitor the reference status under optimal growth conditions. Next, the PFR was connected to the STR for circulating cells without feeding glucose and oxygen in the PFR (Figure 1c). Through this combinatorial setting, cells repeatedly faced glucose and oxygen starvation for 2.6 min, after staying in the well-defined limitation zone in the STR for 6.2 min. Further, five residence times later, the culture was sampled from STR and five PFR ports simultaneously. DOT was monitored continuously in the STR, at the bottom, and at the top of the PFR using oxygen probes (PreSens). STR-PFR scale-down experiments were performed as biological duplicates.

2.6 | Metabolite quantification

Concentrations of glucose, gluconate, and 2-ketogluconate in culture supernatants were determined using a DIONEX UltiMate 3000 High-Performance Liquid Chromatography System (Thermo Fisher Scientific) with an ISERA Metab AAC column 300 × 7.8 mm^2 separation column (particle size: 10 µm, ISERA GmbH). Elution was performed with 5 mM H_2SO_4 at a flow rate of 0.6 ml min^{-1} at 40°C.

For the analysis of samples from STR-PFR cultivations, gluconate and 2-ketogluconate were quantified using isocratic HPLC equipped with a RI detector (1200 Series, Agilent) and a Rezex ROA-Organic Acid H^+ (300 × 7.8 mm^2) column (Phenomenex) at 50°C with a flow of 0.4 ml min^{-1} 5 mM H_2SO_4. Furthermore, glucose concentration was detected separately using an enzymatic assay (r-biopharm AG).

2.7 | Quantification of rhamnolipids

RLs were quantified using reversed-phase HPLC-CAD (Ultimate 3000 with a Corona Veo Charged Aerosol Detector, Thermo Fisher Scientific; NUCLEODUR C18 Gravity 150 × 4.6 mm^2 column, particle size: 3 µm, Macherey-Nagel GmbH & Co. KG). The applied method has been described previously (Bator, Wittgens, et al., 2020). Aqueous samples were adjusted to pH 7 with 1 M KOH, if necessary, to avoid quantification bias. For sample preparation, acetonitrile was added in volumes equal to the aqueous samples for protein precipitation. After mixing and incubation at 4°C for more than 4 h, the samples were centrifuged (21,000*g*, 3 min) and filtered (Phenex RC syringe filters, 0.2 µm, *d* = 4 mm, Phenomenex). For samples drawn from organic phases, the ethyl decanoate was evaporated at 20 mbar, 60°C, and 1400 rpm (ScanSpeed 40 attached to ScanVac Coolsafe 110-4, both Labogene ApS, and Chemistry Hybrid Pump RC 6, vacuubrand GmbH & Co. KG). Appropriate volumes of a 50% acetonitrile – double distilled water solution were applied to resolve dry residuals and filtered subsequently (Phenomenex).

2.8 | Nucleotide analysis

A volume of 2 ml biosuspension was added to 0.5 ml precooled (−22°C) perchloric acid (35% v/v) containing 80 µM EDTA and incubated for 15 min at 6°C while shaking (Cserjan-Puschmann et al., 1999). The sample preparation and analysis were performed according to Löffler et al. (2016). After neutralization, the samples were centrifuged (15 min, 4°C, 7000*g*), and the supernatant was analyzed via HPLC (1200 Series, Agilent) using an RP-C18 phases column (Supercosil™ LC-18-T, 3 µm, 150 × 4.6 mm^2) and a diode array detector. Concentrations of AMP, ADP, ATP, and ppGpp were normalized by dry biomass, and the adenylate energy charge (AEC) was calculated using the approach of Atkinson (1968), Equation (1). Statistical significance was evaluated by ANOVA or two-sided *t*-test.

$$AEC = \frac{ATP + 0.5 \cdot ADP}{AMP + ADP + ATP} \quad (1)$$

2.9 | Biomass quantification

Cell dry weight was quantified by centrifuging 1 ml of sampled fermentation broth at 21,300*g* and 4°C for 5 min (Centrifuge 5430R, Eppendorf AG). The supernatant was discarded, and the cells were washed by resuspending the pellet in 1 ml deionized water. After another centrifugation, the cell suspension was transferred to pre-dried and pre-weighed glass vials and incubated at 80°C. Dried samples were weighed to determine the cell dry weight. For weighing, precise micro balances were used (for STR cultivations: NewClassic MF MS105DU, Mettler Toledo; error: 0.015 mg; for STR-PFR cultivations: XP26 DeltaRange, Mettler Toledo; error: 0.008 mg). Per point of time and per biological replicate, four technical replicates were measured. Evaluation of this method revealed an error of approximately 15% for biomass titers <0.2 g L^{-1}, which is reduced to <5% for biomass titers of >0.5 g L^{-1}, considering biological and technical replicates.

2.10 | Untargeted proteomics

Samples were drawn as technical duplicates from each STR cultivations of *P. putida* KT2440 SK4 at the different applied conditions

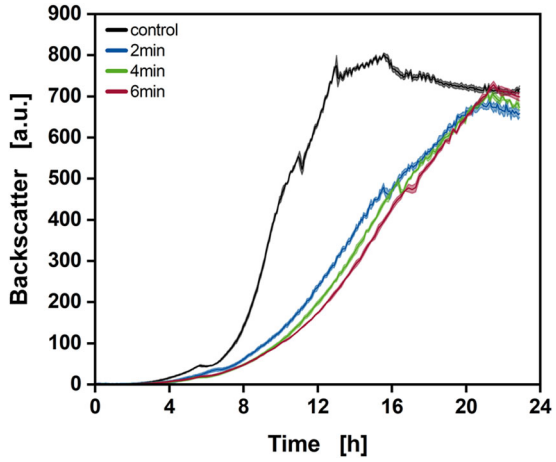

FIGURE 2 Backscatter signal throughout cultivations of *Pseudomonas putida* KT2440 in microtiter plates. A control cultivation, which was continuously shaken at 1200 rpm (black), is compared to alternating shaking frequencies of 1200 rpm and 200 rpm at intervals of 2 min (blue), 4 min (green), and 6 min (red). a.u. = arbitrary units. Shaded areas represent the standard deviation of measurements from five independent experiments

performed in biological duplicates. The control cultures were sampled at t_1 = 7.6 h, whereas the cultures subjected to 2 min oscillations were sampled at t_1 = 7.6 h and again at t_2 = 11.9 h, shortly before glucose depletion. About 10 ml of cultivation broth were sampled in pre-chilled (−20°C) reaction tubes, subsequently centrifuged (5000*g*, 10 min, 4°C), and washed with 0.9% NaCl (4°C). Cell pellets were rapidly cooled in liquid nitrogen and stored at −20°C until further analysis.

The cell pellets were suspended in lysis buffer containing 50 mM potassium phosphate buffer (pH 8.0), 2 mM EDTA, 2 mM 1,4-dithiothreitol (DTT), and supplemented with cOmplete protease inhibitor cocktail (1697 498, Roche Applied Science). Cell suspensions were disrupted in a Precellys System (Bertin Technologies SAS) using 0.1–0.2 mm glass beads plus two glass beads with 5 mm diameter for 30 s at maximum frequency was repeated two more times. The supernatant containing protein fractions was collected and frozen at −20°C until further analysis. Concentrations of proteins in crude extracts were measured using a Bradford assay (B6916, Sigma-Aldrich) with BSA as standard. According to previously described methods (Voges & Noack, 2012), the resulting crude extracts were then applied for untargeted LC-MS/MS measurement. Briefly, a maximum of 50 µl of the crude extracts (up to 100 µg total protein) were used for tryptic digestion. Crude extracts were digested with 1 µg trypsin in a total volume of 100 µl for 5 h at 42°C as recommended by the supplier (T7575, Sigma-Aldrich). Peptide solutions were diluted 1:2 with MilliQ H_2O (Millipore, Merck KGaA) before LC-MS measurements. With injected sample volumes of 10 µl, protein amounts of up to 5.0 µg were applied. Peptide mixtures were separated by reversed-phase HPLC (Infinity 1260 HPLC, Agilent Technologies; column at 21°C: 150 × 2.1 mm^2 Ascentis Express® Peptide ES-C18 2.7 µm (53307-U, Sigma-Aldrich); equilibration: 3% B (12 min); gradient B: 3%–40% (70 min), 40% (8 min), 40%–60% (1 min), 60% (10 min); flow: 0.2 ml min^{-1}; A: 0.1% (v/v) formic acid, B: acetonitrile+0.1% (v/v) formic acid) before ESI-MS-TOF (Q-ToF 6600 mass spectrometer, Sciex) measurements. The TripleTOF6600 was operated with CUR: 35, GS1: 50, GS2: 50, IS: 5500, TEM: 450, and DP: 120. The variable width Q1 windows were monitored in a non-scheduled manner during the elution under the above-specified parameters. SWATH window width was calculated with SWATH Variable Window Calculator_V1.0. The autosampler was set to ±6°C. Data acquisition and peak integration were performed using the software PeakView 2.1 (Sciex), while proteins were identified with the software ProteinPilot 5.1 (Sciex). Marker View software (Sciex) was used for *t*-test analysis.

3 | RESULTS

3.1 | Periodic oxygen starvation leads to reduced growth rates in microtiter plate cultivations

MTP cultivations were performed to assess the influence of alternating shaking frequencies and a resulting oscillation of the OTR on the growth behavior of wild-type *P. putida* KT2440. Shaking intervals of 2 min, 4 min, and 6 min at 200 rpm and 1200 rpm were compared to a culture continuously shaken at 1200 rpm.

Online backscatter signals revealed prolongations of the cultivation time until the stationary phase was reached when the culture was subjected to oscillation (Figure 2). While the continuously shaken culture entered the stationary phase after 13 h, the cultivation time of the oscillating cultures was extended to 20.8, 21.2, and 21.5 h for the intervals of 2 min, 4 min, and 6 min, respectively. Although all durations of cultivations differ significantly (all *p*-values < 0.05), the growth retardation was only minorly influenced by increased durations of shaking intervals, but primarily by the presence of oscillation itself. This is also reflected in the calculated growth rates during exponential phases of each set of cultivations. The maximal growth rates were determined in the latter part of the cultivations at backscatter signals (BS) > 100 to avoid technical bias (Figure a1). Obtained maximal growth rates for the control cultivations (μ_{ctrl} = 0.70 ± 0.01 h^{-1}) were approximately 2.6-fold higher compared to growth rates of all cultures subjected to oscillation (μ_{osc} = 0.27 ± 0.03 h^{-1}). Only transient phases of exponential growth could be determined, especially for the oscillating cultures, potentially indicating an oxygen limitation. However, although maximal backscatter signals of all cultivation conditions differed significantly (*p*-values < 0.05), generally similar values for all oscillations ($BS_{max,2min}$ = 683 ± 12 a.u., $BS_{max,\ 4min}$ = 707 ± 7 a.u., $BS_{max,\ 6min}$ = 728 ± 14 a.u.) were reached, being only slightly lower than the maximal backscatter signal of the continuously shaken control cultivations ($BS_{max,ctrl}$ = 770 ± 25 a.u.). Therefore, a decelerated growth but similar final biomass titers were concluded when *P. putida* KT2440 was subjected to oscillating OTRs.

The cultivations in the microtiter scale were influenced when subjected to oscillations in shaking frequencies leading to alternating OTR_{max}. In the described cultivations, only the online backscatter signal was accessible, thus there was no information about the DOTs

at different shaking frequencies. MTPs with integrated DOT optodes (John et al., 2003) could have given estimates. However, DOT signals respond to the oscillation in a delayed manner, and measurements could not have been synchronized to the shaking intervals. In addition, a shaken culture in microtiter scale needs validation to be comparable to cultivations in STRs (Marques et al., 2010). To gain more detailed information on the performance of *P. putida* KT2440 at oscillating oxygen availability, STR cultivations allowing to access several on- and offline signals were performed. Here, potential metabolic shifts indicated by stagnating increase in backscatter signal during the cultivations in MTPs can be elucidated by performing sampling and metabolite quantification during STR cultivations.

3.2 | Oscillation of dissolved oxygen tension decelerates growth in STRs

For a more detailed characterization of the effects a temporary and repeated shortage of oxygen availability has on *P. putida* KT2440, STR cultivations were performed. Repeated oxygen limitation during STR cultivations was induced by oscillating aeration and agitation between high and low setpoints. Here, intervals of 2 min and 4 min were investigated.

The duration until carbon source depletion was prolonged for both oscillating cultures compared to the control as indicated by a steep increase of the DOT signals and the measured substrate concentrations at sampling points (Figure 3a–c). All carbon in the control culture was consumed within 8.7 h, whereas carbon source in the oscillating cultures with 2 min and 4 min of oscillation was depleted after 12.8 h and 13.6 h, respectively. The prolonged duration is reflected in the specific carbon uptake rates q_S (Table 1). While the difference in cultivation time between well-aerated and oscillating conditions was significant (4.1 h and 4.9 h), increasing the interval of oscillations from 2 min to 4 min prolonged the duration of the cultivations only minorly by 0.8 h. Dissolved oxygen was temporally depleted in either oscillation interval as indicated by the DOT values at low setpoints approaching 0%. However, the culture subjected to 4 min of oscillation experienced temporal oxygen depletion earlier and over a more extended period. For comprehension, Figure 3a–c shows the minimal and maximal values of the DOT and a shaded

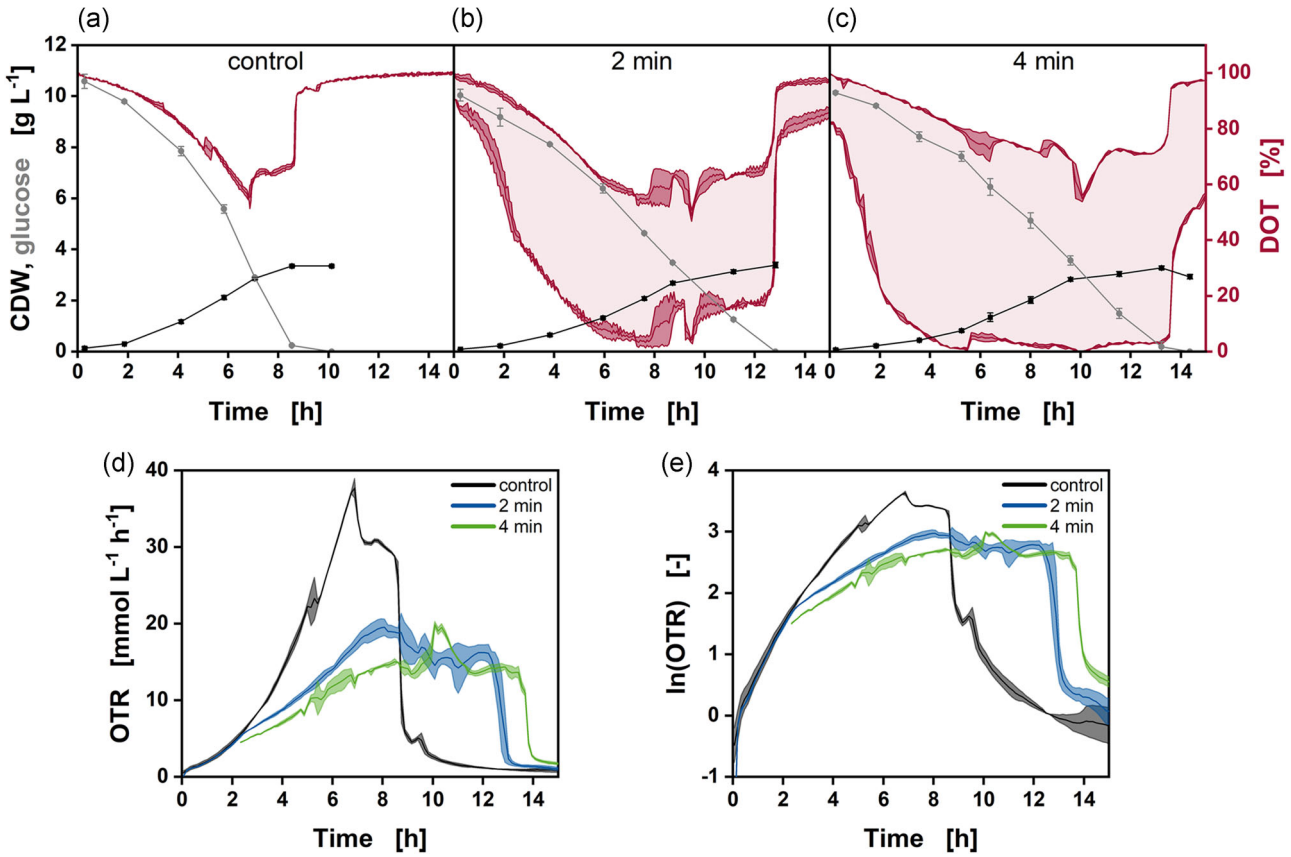

FIGURE 3 Cultivations of *Pseudomonas putida* KT2440 at different intervals of oscillating aeration and agitation. (a–c) CDW (black squares), glucose (gray dots), and DOT (red line) over the cultivation time for (a) well-aerated control cultivations, (b) 2 min intervals of oscillation, and (c) 4 min intervals of oscillation. The solid red lines represent minima and maxima of DOT values, the light red shaded area represents the range of DOT values induced by oscillation. (d, e) OTRs and the respective half-logarithmic plot for the control cultivations (black line), 2 min intervals of oscillation (blue line), and 4 min intervals of oscillation (green line). Error bars and darkly shaded areas represent errors derived from two independent experiments. CDW, cell dry weight; DOT, dissolved oxygen tension; OTR, oxygen transfer rate

TABLE 1 Performance indicators for cultivations of wild-type *Pseudomonas putida* KT2440 in STRs at different conditions

Condition[a]	m(lnOTR)[b] [h^{-1}]	q_S[c] [$g\ g_X^{-1}\ h^{-1}$]	$Y_{X/S}$[d] [$g_X\ g^{-1}$]	Gluconate[e] [$g\ L^{-1}$]	2-Ketogluconate[e] [$g\ L^{-1}$]
Control	0.50 ± 0.02	0.65 ± 0.01	0.32 ± 0.01	0.39 ± 0.00	0.50 ± 0.07
2 min	0.27 ± 0.01	0.49 ± 0.02	0.33 ± 0.02	0.45 ± 0.01	0.67 ± 0.02
4 min	0.26 ± 0.01	0.45 ± 0.01	0.30 ± 0.00	0.40 ± 0.03	0.89 ± 0.12

[a]Control represents the well-aerated culture, 2 min and 4 min the respective intervals of aeration and non-aeration.

[b]Slopes were derived via linear regression from OTR signals from 2.3 h to 5.1 h and reflect growth rates.

[c]Specific glucose uptake rates were calculated via linear regression over the first 8 h of cultivation.

[d]Biomass yields were calculated from the maximal cell dry weight and the used substrate.

[e]Data represents maximal values occurring over the entire cultivation.

range, in which DOT values oscillated. Additionally, Figure a2 depicts a close view of a section of Figure 3b to exemplarily illustrate obtained oscillations of the DOT. The biomass signals reflected the differences in time of cultivations between undisturbed and oscillating cultures. Maximal biomass titers are similar, independent of cultivation conditions ($cx_{max,ctrl}$ = 3.36 ± 0.02 g L^{-1}, $cx_{max,2min}$ = 3.39 ± 0.09 g L^{-1}, $cx_{max,4min}$ = 3.29 ± 0.02 g L^{-1}), but were reached after different durations of cultivation, coinciding with the depletion of carbon source.

Assuming an equal demand of oxygen for each cell, thus a linear correlation between growth and OTR, the OTR signals (Figure 3d) indicated a more complex growth behavior than could be derived from the sampled biomass, especially when oscillation was induced. As measurement intervals of the exhaust gas sensors and their response times did not match oscillation intervals, a moving average of the OTR is depicted, causing the signals to not appear oscillating. While the OTR of the well-aerated control cultivation and the oscillation at an interval of 2 min proceeded similarly up to a cultivation time of 2.3 h (data for the 4 min oscillation not available up to a cultivation time of 2.2 h), the signals diverged afterward as the increase in OTR of oscillating cultures decelerated. Linear regression of the OTR signals (Figure 3e) between 2.3 h and 5.1 h revealed the slope of OTR approximately to be reduced by twofold at either oscillation (Table 1), correlating with decreased growth rates of the respective cultures. Peaks and plateaus in the OTR indicate the co-metabolization of gluconate and 2-ketogluconate formed from glucose. The short stagnation of the OTR at 5 h of the control cultivation, which could also be observed in online backscatter signal of the previous cultivation in MTPs, coincided with a co-metabolization of 2-ketogluconate (refer to Figure a3). Notably, while maximal concentrations of gluconate are similar across all cultivations, the maximal concentrations of 2-ketogluconate increased with extended intervals of oscillation (Table 1 and Figure a1). The latter indicates limitations in providing NADH as the cells can circumvent the NADH-dependent ATP synthesis by generating electrons from the oxidation of gluconate to 2-ketogluconate. Integration of the OTR, starting from 2.3 h until carbon was depleted, revealed a comparable demand for oxygen, independent of disturbance ($O_{2\ consumed,\ control}$ = 140.4 ± 1.0 mmol L^{-1}, $O_{2\ consumed,\ 2min}$ = 143.6 ± 2.8 mmol L^{-1}, $O_{2\ consumed,\ 4min}$ = 139.1 ± 3.9 mmol L^{-1}).

In general, the results obtained from MTP cultivations could be confirmed. *P. putida* KT2440 grows at a reduced rate at oscillating oxygen availability, but final biomass titers at complete carbon depletion remain unaltered.

3.3 | *Pseudomonas putida* withstands repeated short-term oxygen starvation

Cultivations of *P. putida* KT2440 in the STR-PFR intended to unravel long- and short-term physiological responses. For the prior, the phenotypical adaptation to inhomogeneities that are likely to occur in industrial-scale bioreactors was studied. For the latter, metabolic short-term responses to sudden oxygen deprivation were monitored. In contrast to the DOT oscillations in the batch STR cultivations, only a fraction of the entire cell population is simultaneously subjected to oxygen and glucose starvation in the STR-PFR, thus rather resembling the conditions inside industrial-scale bioreactors. STR-PFR tests started with installing a steady-state glucose-limited reference (dilution rate: 0.2 h^{-1}, DOT: 5%) characterized as follows: cell dry weight concentration (c_X = 7.3 ± 0.1 g L^{-1}), adenylate energy charge (AEC = 0.84 ± 0.05), glucose uptake rate (q_S = 0.46 ± 0.01 g $g_X^{-1}\ h^{-1}$), oxygen transfer rate (OTR = 58.4 ± 1.7 mmol $L^{-1}\ h^{-1}$), carbon dioxide transfer rate (CTR = 58.8 ± 1.9 mmol $L^{-1}\ h^{-1}$), see Figure 4a–c. Even though DOT was kept relatively low at 5% in the STR, the growth characteristics resemble the physiological state of the culture when DOT was kept above 20% in a previous study (Ankenbauer et al., 2020). After connection of the PFR to the STR, the low dissolved oxygen and the limited supply of glucose in the STR resulted in complete depletion of oxygen (DOT = 0%) and carbon (glucose, gluconate, and 2-ketogluconate below detection limit) at the entrance and the exit of the PFR, thus creating a transient anaerobic regime under the absence of external carbon (residence time of cells in the PFR τ_{PFR} = 2.6 min).

After additional five residence times under transient dual limitation, cells were sampled to compare physiological parameters with the reference state. *P. putida* showed stable long-term growth performance since phenotypical steady-state parameters were similar to the reference condition despite repeatedly facing starvation zones (Figure 4a–c). Only the energy charge of the cells dropped, however

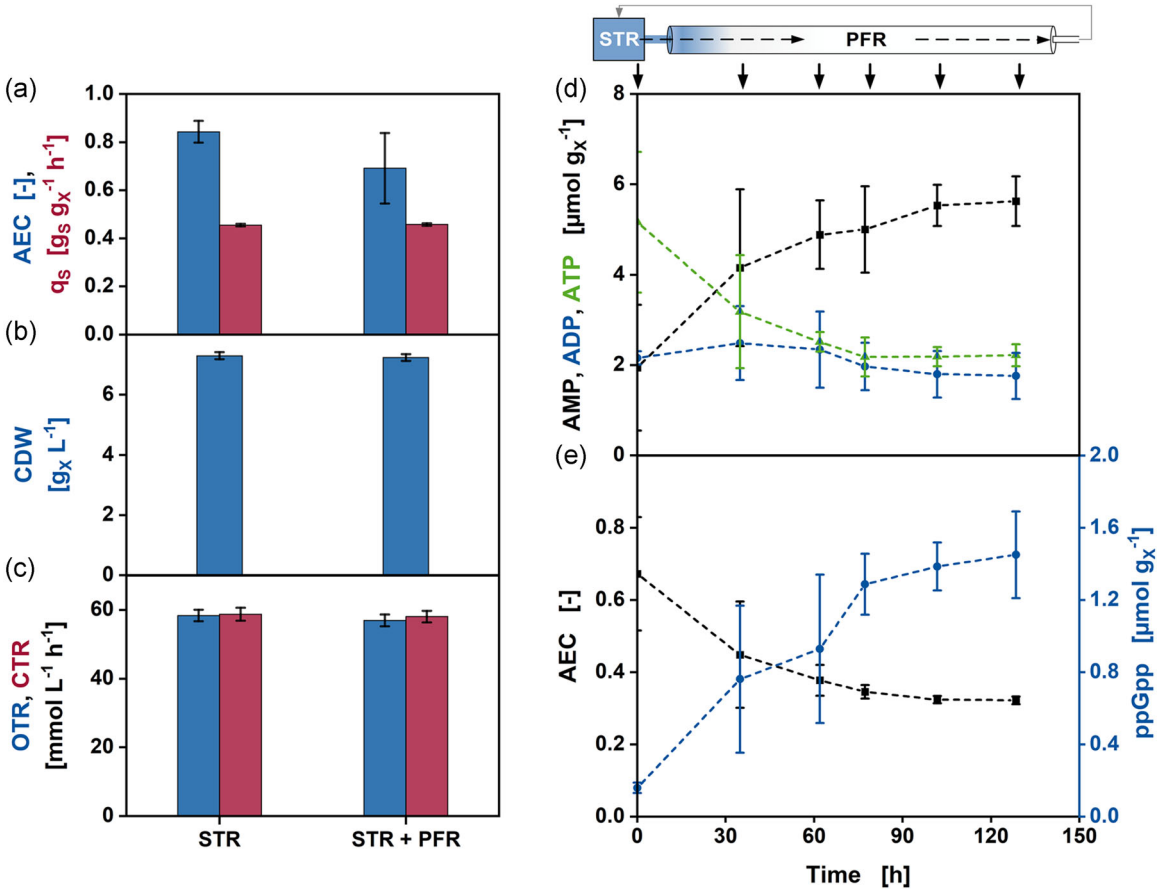

FIGURE 4 (a–c) Long-term response of *Pseudomonas putida* KT2440 to repeated transient oxygen and glucose starvation. (a) Adenylate energy charge (AEC, blue) and glucose uptake rate (qS, red), (b) cell dry weight concentration (CDW, blue), (c) oxygen transfer rates (OTRs, blue), and carbon dioxide transfer rates (CTRs, red). (d, e) Short-term response of *P. putida* KT2440 to transient oxygen and glucose starvation inside the PFR with (e) intracellular AMP (black squares), ADP (blue circles), and ATP (green triangles) concentrations; (f) AEC (black squares) and intracellular ppGpp concentration (blue circles). Error bars represent maximum and minimum values from biological duplicates

not significantly (*t*-test *p*-value > 0.05), from the reference value of 0.84 ± 0.05 to 0.69 ± 0.15.

The short-term response to the dual starvation was monitored by simultaneously sampling via the five PFR ports and the STR port at the second steady-state. The energetic condition of the cells was affected severely due to oxygen and glucose starvation. The AMP level almost doubled from 1.94 ± 1.39 to 5.63 ± 0.55 µmol g_X^{-1}, (*p*-value < 0.05) whereas the ATP level nearly halved from 5.16 ± 1.56 to 2.21 ± 0.24 µmol g_X^{-1} (*p*-value < 0.05) at the exit of the PFR in contrast to the undisturbed cells in the STR (Figure 4d). This resulted in a significant (*p*-value < 0.05) drop of the energy charge (AEC) of the cells from 0.69 ± 0.15 to a critically low level of 0.32 ± 0.01 at the exit of the PFR (Figure 4e). Concomitantly, the intracellular concentration of the stringent response alarmone ppGpp increased significantly from 0.16 ± 0.03 to 1.45 ± 0.24 µmol g_X^{-1} with progressing exposure to dual limitation. However, no significant change of intracellular ADP levels (*p*-value > 0.05) was observed. Even though *P. putida* cells showed severe metabolic reactions to short-term starvation of oxygen and glucose, their overall growth performance was not negatively affected.

3.4 | Exemplary production of rhamnolipids results in unaltered final titers at oscillating DOTs

The effect of oxygen limitation on the production capacity of *P. putida* KT2440 was also assessed, with rhamnolipids serving as an exemplary product. For this, *P. putida* KT2440 SK4, previously engineered to enable rhamnolipid synthesis (Tiso et al., 2020), was cultivated in STRs, again subjected to oscillating aeration and agitation. In addition, ethyl decanoate was added to the cultivation broth as an *in situ* extractant, and the pH was set to 6 to avoid severe foaming. Both the effect of ethyl decanoate and the lowered pH on growth and production have been described previously (Demling et al., 2020).

Similar to the STR cultivations performed with wild-type *P. putida* KT2440, the duration of the cultivation until depletion of the carbon source was prolonged at oscillating oxygen availability as indicated by the sudden increase of the DOT and the offline measurements of glucose (Figure 5a,b). However, the prolongation of cultivations was lowered to 1.5 h compared to cultivations of the wild-type *P. putida* KT2440 (4.1 h prolongation at 2 min

oscillation intervals), where no organic solvent as a second liquid phase was present. The DOT signal of the cultivation at oscillating conditions did not reach values as low as the culture of wild-type *P. putida* KT2440. As the addition of organic solvents has been proven beneficial for enhancing the mass transfer coefficient of oxygen in emulsified two-liquid phase fermentations (van Sonsbeek et al., 1993), the added ethyl decanoate might have resulted in increased oxygen availability and an attenuated oscillation. Here, with increasing RLs and biomass concentrations throughout the cultivation, the extent of this effect would be highly dynamic, depending on different proposed mechanisms. In addition, the presence of surfactants itself has an effect on the mass transfer, which is highly dependent on the type of surfactant and its concentration (Lebrun et al., 2021). Further, the lowered pH was shown to reduce growth rates of *P. putida* KT2440 (Demling et al., 2020), thus the oxygen demand of the cells is lower over time compared to the wild-type, in turn potentially resulting in a higher DOT. In addition, it is questionable how much of the measured oxygen is accessible for the microorganisms as oxygen dissolved in ethyl decanoate might be inaccessible, but the average of DOTs in both phases was measured by the optical probe.

While gluconate accumulated similarly at both cultivation conditions, nearly no 2-ketogluconate was detected (Table 2 and Figure a2). This might be due to a higher demand of glucose-6-phosphate (G6P) required to produce activated dTDP-L-rhamnose, which is transferred to HAAs by the rhamnosyltransferase RhlB to form mono-RLs. Previously, the carbon flux via the rhamnose pathway was revealed to be increased by 300% in a rhamnolipid producing *P. putida* KT2440, thus creating the mentioned demand (Tiso et al., 2016). The presence of ethyl decanoate severely impeded the determination of biomass concentration via gravimetry or spectroscopy. Therefore, exhaust gas measurements were used to calculate the moving average of OTRs as it is dependent on biomass and thus growth. Whereas the OTR of the non-oscillating cultivation generally revealed an exponential incline between approximately 1.7 h and 8 h (Table 2), a two-staged growth behavior was observed for *P. putida* KT2440 SK4 subjected to oscillations. Between cultivation times of approximately 1.7 h and 5.1 h, the OTR of the cultures exhibited an exponential incline, however, growth appears to be linear thereafter (Figure 5c,d), indicating a limitation. Similar to the cultivation of the wild-type *P. putida* KT2440, integration of the OTR lead to comparable demand of oxygen until the carbon source was depleted

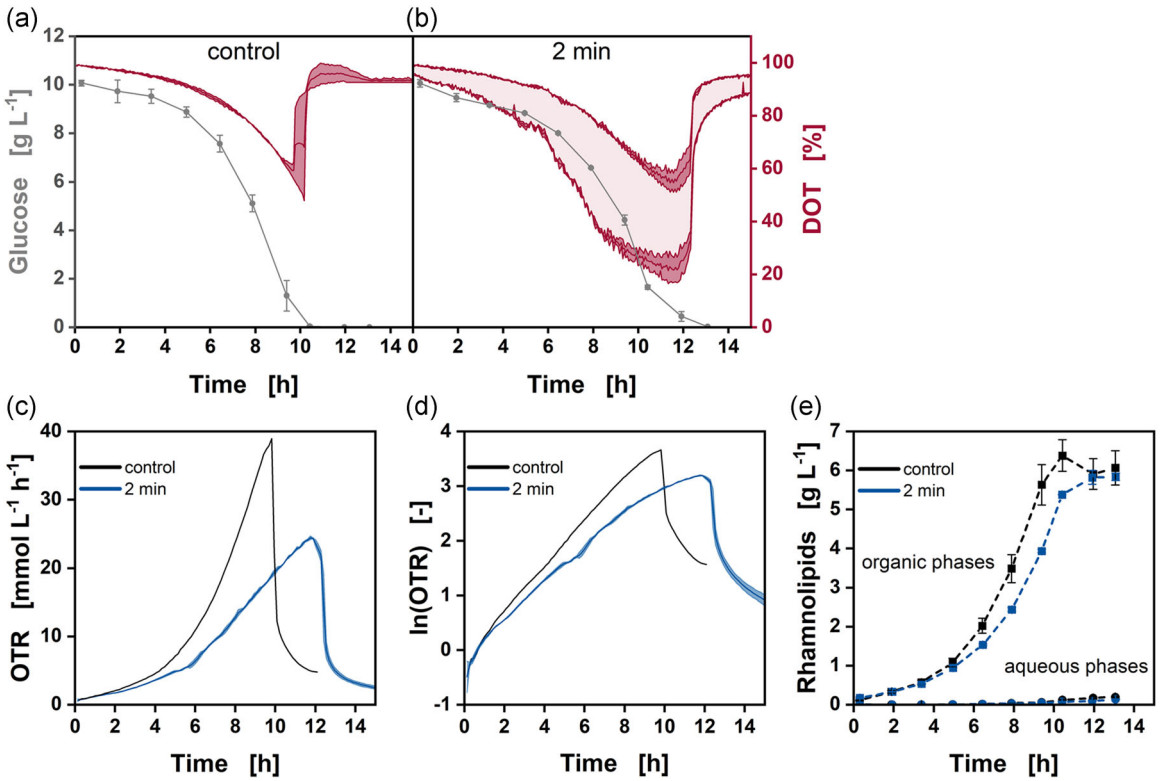

FIGURE 5 Comparison of cultivations of *Pseudomonas putida* KT2440 SK4 at different intervals of oscillating aeration and agitation. (a, b) Glucose (gray dots) and DOT (red line) over the cultivation time for (a) well-aerated control cultivations and (b) 2 min intervals of oscillation. The solid red lines represent averages of minima and maxima of DOT values. The light red shaded area represents the range of DOT values induced by oscillation. (c, d) OTRs and the respective half-logarithmic plot for the control cultivations (black line) and 2 min intervals of oscillation (blue line). (e) Average rhamnolipid titers in aqueous and organic phases for the control (black dashed lines) and 2 min intervals of oscillation (blue dashed lines). Error bars and darkly shaded areas represent errors derived from two independent experiments. For the control cultivation, only one exhaust gas measurement was recorded. DOT, dissolved oxygen tension; OTR, oxygen transfer rate

TABLE 2 Performance indicators for cultivations of *Pseudomonas putida* KT2440 SK4 in STRs at different conditions

Condition[a]	m(lnOTR)[b] [h^{-1}]	$Y_{P/S}$[c] [g_{RL} g^{-1}]	STY[d] [g_{RL} L^{-1} h^{-1}]	Gluconate[e] [g L^{-1}]	2-Ketogluconate[e] [g L^{-1}]
Control	0.42	0.12 ± 0.01	0.11 ± 0.01	0.85 ± 0.01	0.01 ± 0.00
2 min	0.35 ± 0.01	0.11 ± 0.00	0.09 ± 0.00	0.79 ± 0.01	0.02 ± 0.00

[a]Control represents the continuously aerated culture, 2 min intervals of aeration and non-aeration.

[b]Slopes were derived via linear regression from OTR signals from 1 to 5.1 h and reflect growth rates.

[c]Product yields were calculated from the maximal RL concentrations in the organic phase and the aqueous phase normalized by their respective volumes and the used substrate.

[d]Space-time yields were calculated from the maximal RL concentrations in the organic phase and in the aqueous phase normalized by their respective volumes and the time.

[e]Data represents maximal values occurring over the entire cultivation.

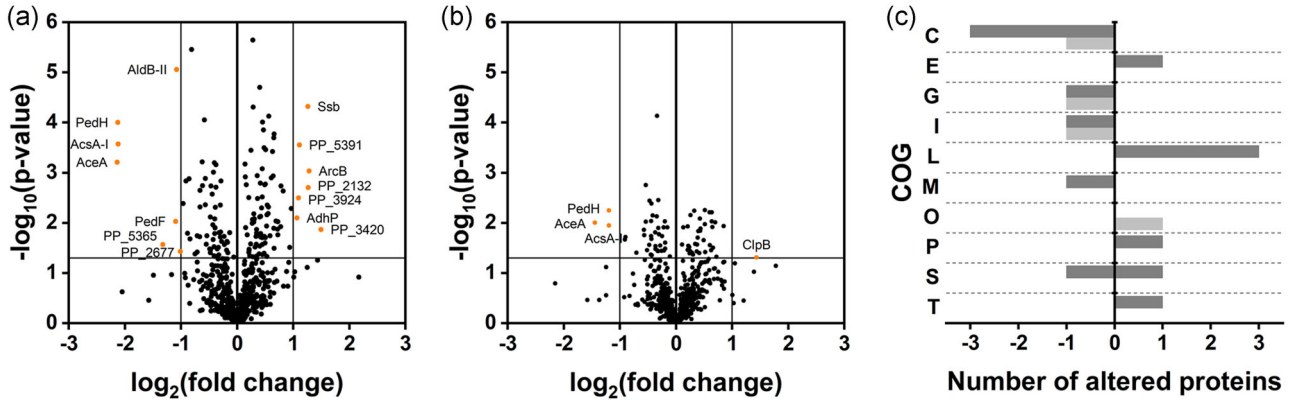

FIGURE 6 Relative differences in abundances of detected proteins in *Pseudomonas putida* KT2440 SK4 subjected to oscillating DOT compared to undisturbed control cultivations. (a) Volcano plot to determine significantly altered proteins at t_1. Cutoff values were set to a $\log_2$ fold change of 1 and a *p*-value of 0.05. Orange data points represent proteins of significantly altered abundance. (b) Analog to (a) for t_2. (c) Grouping of altered proteins according to COGs, which were retrieved via eggnog 5.0.0, for t_1 (dark gray bars) and t_2 (light gray bars). Positive *x*-values represent the number of proteins with increased abundance, while negative numbers represent the number of proteins with reduced abundance. COGs: C – Energy production and conversion, E – Amino acid transport and metabolism, G – Carbohydrate transport and metabolism, I – Lipid transport and metabolism, L – Replication, recombination, and repair, M – Cell wall/membrane/envelope biogenesis, O – Posttranslational modification, protein turnover, and chaperones, P – Inorganic ion transport and metabolism, S – Unknown function, T – Signal transduction mechanism. Proteins and according information are listed in Table a1. COG; cluster of orthologous groups; DOT, dissolved oxygen tension

($O_{2\ consumed,control}$ = 120.7 mmol L^{-1}, $O_{2\ consumed,2min}$ = 123.4 ± 0.6 mmol L^{-1}).

The bulk of produced rhamnolipids was extracted from the organic phases (Figure 5e). Comparing titers of the two cultivation conditions, the same temporal offset recorded in the exhaust gas data was observed. Despite slower production in the cultivation subjected to oscillations, maximum titers were comparable, thus indicating no significant adverse effects of repeated oxygen limitations on the carbon yield, but rather on the space-time yield (Table 2), thus agreeing with the prolonged cultivation time until depletion of the carbon source.

Concluding, the cultivations of *P. putida* KT2440 SK4 in STRs showed that oscillating DOTs do not influence the strain's capacity to produce rhamnolipids, but are similar to the effect on growth results in reduced rates. While this was explicitly studied for the production of rhamnolipids, it remains unclear if it can be generalized for any production of secondary metabolites with recombinant *P. putida* KT2440.

3.5 | *Pseudomonas putida* KT2440 subjected to oscillations alters proteome only minorly

Untargeted proteomics was used to compare samples from the STR cultivations of *P. putida* KT2440 SK4 at the different applied conditions to gain information about intracellular responses to oscillating DOTs. The continuously aerated cultures were sampled once at t_1 = 7.6 h, whereas the cultures subjected to oscillations were sampled at t_1 = 7.6 h and again at t_2 = 11.9 h, shortly before glucose depletion. Only proteins whose abundances were significantly altered at least twofold (*p*-value < 0.05) when subjected to oscillations were considered.

The synthesis of only a minor number of proteins was upregulated or downregulated in cells cultivated at oscillating conditions (Figure 6a,b and Table a1). Seven proteins were at least twofold more abundant, and seven proteins were reduced at least twofold compared to the control. In total, this accounts for only about 2% of all 691 detected proteins. At t_2, this ratio was even further reduced to 0.6% (one upregulated and three downregulated). The relatively low overall alteration indicates that *P. putida* KT2440 does not majorly alter its proteome but can cope with oscillating oxygen availability using its existing set of proteins. When grouping the proteins of changed abundance according to the clusters of orthologous groups (COGs) database (Tatusov et al., 1997) retrieved using eggnog 5.0.0, predominantly proteins of the COG C "Energy production and conversion" were less abundant, whereas mainly proteins associated with COG L "Replication, recombination, and repair" were synthesized at least twofold higher than in the control (Figure 6c).

The protein exhibiting the most severe downregulated synthesis at t_1 and t_2 was the isocitrate lyase (AceA, PP_4116), indicating downregulation of the glyoxylate shunt and lower carbon flux through the TCA cycle. The upregulated synthesis of proteins related to replication, recombination, and repair, chaperones, or stress response (PP_0625, chaperone protein ClpB (t_2 only); PP_0485, single-stranded DNA-binding protein; PP_2132, universal stress protein; PP_3420, sensor histidine kinase (all t_1 only)) indicates *P. putida* KT2440 to be stressed by oscillation.

Further, proteomics data showed a downregulated synthesis of the acetyl-CoA synthase AcsA-I (PP_4487) and several proteins from the *ped* cluster (PP_2675, cytochrome *c* oxidase PedF; PP_2677, hypothetical protein; PP_2679, PQQ-dependent alcohol dehydrogenase PedH; and PP_2680, aldehyde dehydrogenase AldB-II) as well as an upregulated synthesis of the alcohol dehydrogenase AdhP (PP_3839). A change in levels of alcohol dehydrogenases indicates the presence of alcohols, which could potentially be attributed to impurities of the applied ethyl decanoate (≥98% purity) or its de-esterification by *P. putida* KT2440 resulting in ethanol and decanoate. However, in both the control and the oscillating cultivation, ethyl decanoate from the same stock was used. We previously showed that *P. putida* KT2440 could not use ethyl decanoate as a carbon source in the presence of glucose or directly after glucose depletion (Demling et al., 2020). Further, metabolization of ethanol would require the activity of the acetyl-CoA synthase to generate acetyl-CoA from acetate. However, we observed the expression of *acsA-I* to be downregulated, which would result in an accumulation of acetate. Neither acetate nor ethanol was detected in the supernatant.

4 | DISCUSSION

4.1 | *Pseudomonas putida* KT2440 endures temporary oxygen starvation

We studied the influence of temporary oxygen deprivation on the growth of the obligate aerobic *P. putida* KT2440 across different cultivation systems and scales ranging from microtiter to lab-scale reactors simulating large-scale fermenters. In batch cultivations at all scales, the growth behavior appears to follow a similar pattern. When oxygen is temporarily limited, the growth rate of the cells decreases and transitions into linear growth, leading to prolonged cultivation times until carbon source depletion in contrast to well-aerated cultures. However, final biomass titers are comparable. As this phenotype is consistent throughout MTP and STR cultivations, the presented approach of implementing oscillating shaking frequencies to cause repeated oxygen shortage could be applied in similar future studies for estimations on growth behavior before running scale-down experiments in more complex setups. Strikingly, the length of oscillating intervals does not seem to impact the length of cultivation substantially as studied for MTP and STR cultivations for the wild-type *P. putida* KT2440, but rather the occurrence of oscillation causes the observed effect. This might be due to the equal durations of aeration and non-aeration within each periodic cycle. However, preliminary results from STR cultivations with unequal durations of each condition showed similar effects. Randomized durations might give different results and could be more accurate in simulating the transient conditions cells encounter due to their trajectory through large-scale reactors (Haringa et al., 2016; Kuschel et al., 2017). In the STR-PFR scale-down experiments, the overall growth performance of *P. putida* KT2440 was not impaired by repeated exposure to dual substrate starvation as the cells can reach the set growth rate of 0.2 h^{-1}. Recent CFD simulations revealed several transitions through oxygen and glucose starvation zones during 200 s of a bacterial lifeline circulating through a large-scale bioreactor operated as fed-batch (Kuschel & Takors, 2020). Since their study predicted glucose levels mainly below 32 mg L^{-1} even in oxygen restricted zones, our STR-PFR setup, in which cells repeatedly traversed glucose limitation and dual starvation zones mimics large-scale inhomogeneities well enough. In accordance with our results, it was observed that *P. putida* cells achieved similar biomass yields and even accelerated the DNA replication when exposed to a critical low DOT at 1.5% compared to optimal conditions in a chemostat culture (Lieder et al., 2016). Contrarily, it was previously shown that final biomass titers of *P. putida* strains were reduced when subjected to a strict oxygen limitation induced by low but constant agitation (Escobar et al., 2016; Rodriguez et al., 2018). As we observed similar final biomass titers in this study, we infer that *P. putida* KT2440 can rapidly recover from oxygen starvation when resupplied with oxygen. This phenotype emphasizes *P. putida*'s outstanding trait to cope with different stress situations due to its versatile metabolism (Chavarría et al., 2013). Further, the RL titers produced at oscillating conditions were comparable to those of well-aerated control cultivations, but space-time yields were decreased. Therefore, we conclude that *P. putida* KT2440 is well suited for large-scale production processes exhibiting gradients in oxygen concentrations, however, at reduced productivity. Advantageously, in contrast to whole-cell biocatalysts capable of fermenting, no undesired byproducts are produced, except for gluconate and 2-ketogluconate, which are in turn metabolized and reused as a carbon source by *P. putida* KT2440. Thereby, carbon

efficiency might be enhanced, and downstream processing might be facilitated. It needs to be validated if these conclusions can be transferred to production processes for products other than RLs.

4.2 | Intracellular mechanisms for coping with repeated oxygen starvation remain ambiguous

While growth and production appear to be robust, the distinct intracellular mechanisms for coping with repeated oxygen starvation have to be discussed further. The results from the STR-PFR scale-down experiments show that *P. putida* cells are unable to quickly recover their energy charge when facing sudden glucose and oxygen starvation. This contrasts with cells facing only glucose deprivation. It was recently observed that *P. putida* could generate energy equivalents from intracellularly accumulated 3-hydroxyalkanoates (3-HA) once external glucose is exhausted (Ankenbauer et al., 2020). Furthermore, the authors detected significant transcriptomic upregulation of genes encoding for amino acid and glycogen catabolic enzymes in glucose starving cells inside the PFR. Thus, *P. putida* is well equipped with different metabolic strategies to counteract sudden carbon starvation and, consequently, can sustain its energy charge. However, when facing dual starvation of glucose and oxygen, cells cannot properly balance their energy demand as the energy charge drops significantly from 0.7 below 0.4. Notably, energy charges above 0.7 are reported for growing *P. putida* cells (Chapman et al., 1971; Vallon et al., 2015). We assume that the lack of oxygen disrupts the electron transport in the respiratory chain that is crucial to oxidize the energy equivalents NADH and $FADH_2$ and create a proton gradient to drive the ATP synthase. In accordance with this hypothesis, the intracellular ATP level decreased, whereas AMP accumulated in the cells during transient oxygen and glucose starvation. Furthermore, increased pools of ppGpp were also found in glucose starving *E. coli* (Löffler et al., 2016) and *P. putida* cells (Ankenbauer et al., 2020). This alarmone is tightly linked to the stringent response machinery and serves as a crucial signaling molecule during starvation stress (Hauryliuk et al., 2015; Traxler et al., 2011). However, additional analytical methods such as transcriptomics and intracellular 3-HA quantification need to be applied to unveil transcriptional and metabolic responses to the installed anaerobic conditions.

In our proteome data, we detected an altered abundance of only a minor number of proteins. This contrasts with previous comparative proteomic studies of *P. putida* KT2440 subjected to stressors, like organic solvents and heavy metals (Miller et al., 2009; Santos et al., 2004), and dual limitations in carbon and phosphorus (Możejko-Ciesielska & Serafim, 2019) or iron deprivation (Heim et al., 2003), all showing a higher number of proteins with altered abundance. Our data indicates that the synthesis of the isocitrate lyase was downregulated when *P. putida* KT2440 encountered oscillating DOTs. Previously, it has been shown that a deletion of the isocitrate lyase resulted in an increased polyhydroxyalkanoates (PHA) production, assumed to cause a lower carbon flux through the tricarboxylic acid cycle, thus increasing the pool of acetyl-CoA potentially used for PHA synthesis (Klinke et al., 2000). *P. putida* KT2440 is known to produce PHA when encountering stress caused by changing environmental conditions, for example, repeated carbon starvation or transition to nitrogen starvation (Ankenbauer et al., 2020; Obruca et al., 2018). We detected a higher abundance of proteins associated with stress response, but it is unknown if stress caused by oxygen limitation or oscillating oxygen availability induces PHA production, which was not quantified in this study. In this case, a likewise increase of RL titers could be expected as 3-hydroxyalkanoate (3-HA) is the precursor for both PHA and RLs, however, our data show no change in RL titer when cells were subjected to oscillations.

Moreover, the proteomics studies revealed a downregulated synthesis of several proteins encoded within the *ped* cluster. Recently, proteins of the *ped* cluster have been shown to be involved in the oxidation of alcohols by *P. putida* KT2440 (Bator, Karmainski, et al., 2020; Li et al., 2020; Thompson et al., 2020). Subsequently, using cytochrome *c*, electrons are transferred to the cytochrome *c* oxidase (PP_2675, PedF), which was also less abundant here, in turn reducing O_2 as part of the respiratory electron transfer chain (García-Horsman et al., 1994; Wehrmann et al., 2020). The downregulation of the *ped* can thus be reasoned with the temporary low abundance of molecular O_2, impeding the functionality of PedF and potentially the PQQ biosynthesis pathway, which requires molecular O_2 itself. As the regulation of the whole cluster seems to be multi-leveled and interconnected (Bator, Karmainski, et al., 2020; Thompson et al., 2020), similar expression levels of individual genes of the cluster might be caused by the same trigger such as limited availability of molecular O_2. The higher abundance of NAD^+-dependent AdhP indicates its function as a complementary alcohol dehydrogenase, which might be favored over PedH at shortage of NADH, which is suggested by the increasing 2-ketogluconate concentrations in the wild-type cultivations. In fact, deletion of both *pedH* and *adhP* caused *P. putida* KT2440 to lose its ability to metabolize short-chain alcohols, while single deletion strains retained functionality (Thompson et al., 2020). However, if altered abundances of proteins of the *ped* cluster and AdhP are solely due to oscillating DOTs or if the presence of an organic solvent triggers their synthesis in the first place, remains unclear.

In general, the presented data suggests that *P. putida* KT2440 can cope with repeated oxygen starvation at the cost of its energy charge but can partially restore it when oxygen becomes available again without majorly altering its proteome. Further studies on the transcriptome and proteome in combination with the quantification of PHAs need to be conducted to elucidate the intracellular coping mechanisms in more detail.

5 | CONCLUSION

Oxygen starvation zones accompanied by other substrate gradients caused by mixing inhomogeneities are likely to occur in industrial-scale bioreactors. In this study, we demonstrate the ability of *P. putida* KT2440 classified as an obligate aerobic microorganism to

withstand temporary oxygen limitations, even with simultaneous carbon starvation. The growth performance of the wild-type strain is not affected significantly by repeated exposure to oxygen starvation. Remarkably, this was confirmed in different scales and cultivation systems, different cultivation media, as well as different laboratories. Moreover, the rhamnolipid production strain accumulated similar product titers during oxygen oscillation compared to the well-aerated reference process. As we showed that both, growth and production are robust when cells are subjected to temporary oxygen starvation, the suitability of *P. putida* KT2440 for industrial-scale production processes was affirmed.

ACKNOWLEDGMENTS

The project on which this report is based was funded by the German Federal Ministry of Education and Research under the funding code 031B0350B. The laboratory of LMB was partially funded by the Deutsche Forschungsgemeinschaft (DFG, German Research Foundation) under Germany's Excellence Strategy within the Cluster of Excellence FSC 2186 "The Fuel Science Center." The research contribution from the Institute of Biochemical Engineering was gratefully funded by the European Union's Horizon 2020 research and innovation program under grant agreement no. 635536. The responsibility for the content of this publication lies with the authors. The authors thank Florian Röck and Lorenzo Favilli for experimental support and Roman Jansen and Laura Grabowski for logistics regarding proteomics. Open Access funding enabled and organized by Projekt DEAL.

CONFLICT OF INTERESTS

LMB and TT declare that they are inventors of three related patents. (1) L. M. Blank, F. Rosenau, S. Wilhelm, A. Wittgens, T. Tiso, "Means and methods for rhamnolipid production," HHU Düsseldorf University, TU Dortmund University, 2013 (WO 2013/041670 A1), (2) L. M. Blank, B. Küpper, E. M. del Amor Villa, R. Wichmann, C. Nowacki, "Foam adsorption," TU Dortmund University, 2013 (WO 2013/087674 A1), and (3) L. M. Blank, T. Tiso, A. Germer, "Extracellular production of designer hydroxyalkanoyloxy alkanoic acids with recombinant bacteria," RWTH Aachen University, 2015 (WO2017006252A1). Apart from that, the authors declare that the research was conducted in the absence of any commercial or financial relationships that could be construed as a potential conflict of interest.

AUTHOR CONTRIBUTIONS

MTP and STR batch cultivations, analytics STR cultivations, secondary processing of proteomics data: Philipp Demling. *STR-PFR cultivation*: Andreas Ankenbauer and Philipp Demling. *Analytics STR-PFR cultivations*: Andreas Ankenbauer. *Proteomics measurements and primary processing*: Bianca Klein. *Interpreted results*: Philipp Demling, Andreas Ankenbauer, Bianca Klein, Stephan Noack, Till Tiso, Ralf Takors, and Lars M. Blank. *Drafted the manuscript*: Philipp Demling (all parts despite STR-PFR sections), Andreas Ankenbauer (STR-PFR sections). *Revised and edited the manuscript*: Stephan Noack, Till Tiso, Ralf Takors, and Lars M. Blank. All authors read, corrected, and commented on the manuscript before publication. All authors approved the final manuscript.

DATA AVAILABILITY STATEMENT

The data that support the findings of this study are available from the corresponding author upon reasonable request.

ORCID

Philipp Demling https://orcid.org/0000-0002-0351-1119
Andreas Ankenbauer https://orcid.org/0000-0002-2843-683X
Stephan Noack http://orcid.org/0000-0001-9784-3626
Till Tiso https://orcid.org/0000-0003-4420-5609
Ralf Takors http://orcid.org/0000-0001-5837-6906
Lars M. Blank https://orcid.org/0000-0003-0961-4976

REFERENCES

Ankenbauer, A., Nitschel, R., Teleki, A., Müller, T., Favilli, L., Blombach, B., & Takors, R. (2021). Micro-aerobic production of isobutanol with engineered *Pseudomonas putida*. *Engineering in Life Sciences*, *21*, 1–14. https://doi.org/10.1002/elsc.202000116

Ankenbauer, A., Schäfer, R. A., Viegas, S. C., Pobre, V., Voß, B., Arraiano, C. M., & Takors, R. (2020). *Pseudomonas putida* KT2440 is naturally endowed to withstand industrial-scale stress conditions. *Microbial Biotechnology*, *13*(4), 1145–1161. https://doi.org/10.1111/1751-7915.13571

Askitosari, T. D., Berger, C., Tiso, T., Harnisch, F., Blank, L. M., & Rosenbaum, M. A. (2020). Coupling an electroactive *Pseudomonas putida* KT2440 with bioelectrochemical rhamnolipid production. *Microorganisms*, *8*(12):1959. https://doi.org/10.3390/microorganisms8121959

Atkinson, D. E. (1968). Energy charge of the adenylate pool as a regulatory parameter. Interaction with feedback modifiers. *Biochemistry*, *7*(11), 4030–4034. https://doi.org/10.1021/bi00851a033

Bagdasarian, M., Lurz, R., Rückert, B., Franklin, F., Bagdasarian, M. M., Frey, J., & Timmis, K. N. (1981). Specific-purpose plasmid cloning vectors II. Broad host range, high copy number, RSF 1010-derived vectors, and a host-vector system for gene cloning in *Pseudomonas*. *Gene*, *16*(1), 237–247. https://doi.org/10.1016/0378-1119(81)90080-9

Bator, I., Karmainski, T., Tiso, T., & Blank, L. M. (2020). Killing two birds with one stone – Strain engineering facilitates the development of a unique rhamnolipid production process. *Frontiers in Bioengineering and Biotechnology*, *8*, 899. https://doi.org/10.3389/fbioe.2020.00899

Bator, I., Wittgens, A., Rosenau, F., Tiso, T., & Blank, L. M. (2020). Comparison of three xylose pathways in *Pseudomonas putida* KT2440 for the synthesis of valuable products. *Frontiers in Bioengineering and Biotechnology*, *7*, 480. https://doi.org/10.3389/fbioe.2019.00480

Bednarz, A., Weber, B., & Jupke, A. (2017). Development of a CFD model for the simulation of a novel multiphase counter-current loop reactor. *Chemical Engineering Science*, *161*, 350–359. https://doi.org/10.1016/j.ces.2016.12.048

Bellou, S., Makri, A., Triantaphyllidou, I.-E., Papanikolaou, S., & Aggelis, G. (2014). Morphological and metabolic shifts of induced *Yarrowia lipolytica* by alteration of the dissolved oxygen concentration in the growth environment. *Microbiology*, *160*(4), 807–817. https://doi.org/10.1099/mic.0.074302-0

Blank, L. M., Narancic, T., Mampel, J., Tiso, T., & O'Connor, K. (2020). Biotechnological upcycling of plastic waste and other

non-conventional feedstocks in a circular economy. *Current Opinion in Biotechnology*, *62*, 212–219. https://doi.org/10.1016/j.copbio.2019.11.011

Chapman, A. G., Fall, L., & Atkinson, D. E. (1971). Adenylate energy charge in *Escherichia coli* during growth and starvation. *Journal of Bacteriology*, *108*, 1072–1086.

Chavarría, M., Nikel, P. I., Pérez-Pantoja, D., & de Lorenzo, V. (2013). The Entner–Doudoroff pathway empowers *Pseudomonas putida* KT2440 with a high tolerance to oxidative stress. *Environmental Microbiology*, *15*(6), 1772–1785. https://doi.org/10.1111/1462-2920.12069

Cserjan-Puschmann, M., Kramer, W., Duerrschmid, E., Striedner, G., & Bayer, K. (1999). Metabolic approaches for the optimisation of recombinant fermentation processes. *Applied Microbiology and Biotechnology*, *53*(1), 43–50. https://doi.org/10.1007/s002530051612

Demling, P., Campenhausen, M., von, Grütering, C., Tiso, T., Jupke, A., & Blank, L. M. (2020). Selection of a recyclable *in situ* liquid-liquid extraction solvent for foam-free synthesis of rhamnolipids in a two-phase fermentation. *Green Chemistry*, *22*, 8495–8510. https://doi.org/10.1039/D0GC02885A

Enfors, S.-O., Jahic, M., Rozkov, A., Xu, B., Hecker, M., Jürgen, B., Krüger, E., Schweder, T., Hamer, G., O'Beirne, D., Noisommit-Rizzi, N., Reuss, M., Boone, L., Hewitt, C., McFarlane, C., Nienow, A., Kovacs, T., Trägårdh, C., Fuchs, L., … Manelius, Å. (2001). Physiological responses to mixing in large scale bioreactors. *Journal of Biotechnology*, *85*(2), 175–185. https://doi.org/10.1016/S0168-1656(00)00365-5

Escobar, S., Rodriguez, A., Gomez, E., Alcon, A., Santos, V. E., & Garcia-Ochoa, F. (2016). Influence of oxygen transfer on *Pseudomonas putida* effects on growth rate and biodesulfurization capacity. *Bioprocess and Biosystems Engineering*, *39*(4), 545–554. https://doi.org/10.1007/s00449-016-1536-6

García-Horsman, J. A., Barquera, B., Rumbley, J., Ma, J., & Gennis, R. B. (1994). The superfamily of heme-copper respiratory oxidases. *Journal of Bacteriology*, *176*(18), 5587–5600. https://doi.org/10.1128/jb.176.18.5587-5600.1994

Haringa, C., Tang, W., Deshmukh, A. T., Xia, J., Reuss, M., Heijnen, J. J., Mudde, R. F., & Noorman, H. J. (2016). Euler-Lagrange computational fluid dynamics for (bio)reactor scale down: An analysis of organism lifelines. *Engineering in Life Sciences*, *16*(7), 652–663. https://doi.org/10.1002/elsc.201600061

Hartmans, S., Smits, J. P., van der Werf, M. J., Volkering, F., & de Bont, J. A. M. (1989). Metabolism of styrene oxide and 2-phenylethanol in the styrene-degrading *Xanthobacter* strain 124X. *Applied and Environmental Microbiology*, *55*(11), 2850–2855.

Hauryliuk Vasili, Atkinson Gemma C., Murakami Katsuhiko S., Tenson Tanel, Gerdes Kenn (2015). Recent functional insights into the role of (p)ppGpp in bacterial physiology. *Nature Reviews Microbiology*, *13*(5), 298–309. http://dx.doi.org/10.1038/nrmicro3448

Heim, S., Ferrer, M., Heuer, H., Regenhardt, D., Nimtz, M., & Timmis, K. N. (2003). Proteome reference map of *Pseudomonas putida* strain KT2440 for genome expression profiling: Distinct responses of KT2440 and *Pseudomonas aeruginosa* strain PAO1 to iron deprivation and a new form of superoxide dismutase. *Environmental Microbiology*, *5*(12), 1257–1269. https://doi.org/10.1111/j.1462-2920.2003.00465.x

Hintermayer, S. B., & Weuster-Botz, D. (2017). Experimental validation of in silico estimated biomass yields of *Pseudomonas putida* KT2440. *Biotechnology Journal*, *12*(6), https://doi.org/10.1002/biot.201600720

John, G. T., Klimant, I., Wittmann, C., & Heinzle, E. (2003). Integrated optical sensing of dissolved oxygen in microtiter plates: A novel tool for microbial cultivation. *Biotechnology and Bioengineering*, *81*(7), 829–836. https://doi.org/10.1002/bit.10534

Kampers, L. F. C., van Heck, R. G. A., Donati, S., Saccenti, E., Volkers, R. J. M., Schaap, P. J., Suarez-Diez, M., Nikel, P. I., & Martins dos Santos, Vitor, A. P. (2019). *In silico*-guided engineering of *Pseudomonas putida* towards growth under micro-oxic conditions. *Microbial Cell Factories*, *18*(1), 179. https://doi.org/10.1186/s12934-019-1227-5

Kampers, L. F. C., Koehorst, J. J., van Heck, R. J. A., Suarez-Diez, M., Stams, A. J. M., & Schaap, P. J. (2021). A metabolic and physiological design study of *Pseudomonas putida* KT2440 capable of anaerobic respiration. *BMC Microbiology*, *21*(1), 9. https://doi.org/10.1186/s12866-020-02058-1

Kampers, L. F. C., Volkers, R. J. M., & Martins dos Santos, V. A. P. (2019). *Pseudomonas putida* KT2440 is HV1 certified, not GRAS. *Microbial Biotechnology*, *12*(5), 845–848. https://doi.org/10.1111/1751-7915.13443

Kar, T., Destain, J., Thonart, P., & Delvigne, F. (2012). Scale-down assessment of the sensitivity of *Yarrowia lipolytica* to oxygen transfer and foam management in bioreactors: Investigation of the underlying physiological mechanisms. *Journal of Industrial Microbiology & Biotechnology*, *39*(2), 337–346. https://doi.org/10.1007/s10295-011-1030-8

Käß, F., Junne, S., Neubauer, P., Wiechert, W., & Oldiges, M. (2014). Process inhomogeneity leads to rapid side product turnover in cultivation of *Corynebacterium glutamicum*. *Microbial Cell Factories*, *13*(1):6. https://doi.org/10.1186/1475-2859-13-6

Kensy, F., Zimmermann, H. F., Knabben, I., Anderlei, T., Trauthwein, H., Dingerdissen, U., & Büchs, J. (2005). Oxygen transfer phenomena in 48-well microtiter plates: Determination by optical monitoring of sulfite oxidation and verification by real-time measurement during microbial growth. *Biotechnology and Bioengineering*, *89*(6), 698–708. https://doi.org/10.1002/bit.20373

Klinke, S., Dauner, M., Scott, G., Kessler, B., & Witholt, B. (2000). Inactivation of isocitrate lyase leads to increased production of medium-chain-length poly(3-hydroxyalkanoates) in *Pseudomonas putida*. *Applied and Environmental Microbiology*, *66*(3), 909–913. https://doi.org/10.1128/aem.66.3.909-913.2000

Kuschel, M., Siebler, F., & Takors, R. (2017). Lagrangian trajectories to predict the formation of population heterogeneity in large-scale bioreactors. *Bioengineering*, *4*(2):27. https://doi.org/10.3390/bioengineering4020027

Kuschel, M., & Takors, R. (2020). Simulated oxygen and glucose gradients as a prerequisite for predicting industrial scale performance *a priori*. *Biotechnology and Bioengineering*, *117*(9), 2760–2770. https://doi.org/10.1002/bit.27457

Lai, B., Yu, S., Bernhardt, P. V., Rabaey, K., Virdis, B., & Krömer, J. O. (2016). Anoxic metabolism and biochemical production in *Pseudomonas putida* F1 driven by a bioelectrochemical system. *Biotechnology for Biofuels*, *9*(1), 39. https://doi.org/10.1186/s13068-016-0452-y

Lange, J., Münch, E., Müller, J., Busche, T., Kalinowski, J., Takors, R., & Blombach, B. (2018). Deciphering the adaptation of *Corynebacterium glutamicum* in transition from aerobiosis via microaerobiosis to anaerobiosis. *Genes*, *9*(6):297. https://doi.org/10.3390/genes9060297

Lara, A. R., Galindo, E., Ramírez, O. T., & Palomares, L. A. (2006). Living with heterogeneities in bioreactors. *Molecular Biotechnology*, *34*(3), 355–381. https://doi.org/10.1385/MB:34:3:355

Lattermann, C., Funke, M., Hansen, S., Diederichs, S., & Büchs, J. (2014). Cross-section perimeter is a suitable parameter to describe the effects of different baffle geometries in shaken microtiter plates. *Journal of Biological Engineering*, *8*(1):18. https://doi.org/10.1186/1754-1611-8-18

Lebrun, G., Xu, F., Le Men, C., Hébrard, G., & Dietrich, N. (2021). Gas–liquid mass transfer around a rising bubble: Combined effect of rheology and surfactant. *Fluids*, *6*(2) https://doi.org/10.3390/fluids6020084

Li, W.-J., Narancic, T., Kenny, S. T., Niehoff, P.-J., O'Connor, K., Blank, L. M., & Wierckx, N. (2020). Unraveling 1,4-butanediol metabolism in *Pseudomonas putida* KT2440. *Frontiers in Microbiology*, *11*, 382. https://doi.org/10.3389/fmicb.2020.00382

Lieder, S., Jahn, M., Koepff, J., Muller, S., & Takors, R. (2016). Environmental stress speeds up DNA replication in *Pseudomonas putida* in chemostat cultivations. *Biotechnology Journal*, *11*(1), 155–163. https://doi.org/10.1002/biot.201500059

Limberg, M. H., Joachim, M., Klein, B., Wiechert, W., & Oldiges, M. (2017). pH fluctuations imperil the robustness of *C. glutamicum* to short term oxygen limitation. *Journal of Biotechnology*, *259*, 248–260. https://doi.org/10.1016/j.jbiotec.2017.08.018

Löffler, M., Simen, J. D., Jäger, G., Schäferhoff, K., Freund, A., & Takors, R. (2016). Engineering *E. coli* for large-scale production – Strategies considering ATP expenses and transcriptional responses. *Metabolic Engineering*, *38*, 73–85. https://doi.org/10.1016/j.ymben.2016.06.008

Lorantfy, B., Jazini, M., & Herwig, C. (2013). Investigation of the physiological response to oxygen limited process conditions of *Pichia pastoris* Mut+ strain using a two-compartment scale-down system. *Journal of Bioscience and Bioengineering*, *116*(3), 371–379. https://doi.org/10.1016/j.jbiosc.2013.03.021

Marques, M. P. C., Cabral, J. M. S., & Fernandes, P. (2010). Bioprocess scale-up: Quest for the parameters to be used as criterion to move from microreactors to lab-scale. *Journal of Chemical Technology & Biotechnology*, *85*(9), 1184–1198. https://doi.org/10.1002/jctb.2387

Miller, C. D., Pettee, B., Zhang, C., Pabst, M., McLean, J. E., & Anderson, A. J. (2009). Copper and cadmium: Responses in *Pseudomonas putida* KT2440. *Letters in Applied Microbiology*, *49*(6), 775–783. https://doi.org/10.1111/j.1472-765X.2009.02741.x

Możejko-Ciesielska, J., & Serafim, L. S. (2019). Proteomic response of *Pseudomonas putida* KT2440 to dual carbon-phosphorus limitation during mcl-PHAs synthesis. *Biomolecules*, *9*(12), https://doi.org/10.3390/biom9120796

Nadal-Rey, G., McClure, D. D., Kavanagh, J. M., Cornelissen, S., Fletcher, D. F., & Gernaey, K. V. (2020). Understanding gradients in industrial bioreactors. *Biotechnology Advances*, *46*, 107660. https://doi.org/10.1016/j.biotechadv.2020.107660

Nakazawa, T. (2002). Travels of a *Pseudomonas*, from Japan around the world. *Environmental Microbiology*, *4*(12), 782–786. https://doi.org/10.1046/j.1462-2920.2002.00310.x

Neubauer, P., Haggstrom, L., & Enfors, S. O. (1995). Influence of substrate oscillations on acetate formation and growth yield in *Escherichia coli* glucose limited fed-batch cultivations. *Biotechnology and Bioengineering*, *47*(2), 139–146. https://doi.org/10.1002/bit.260470204

Neubauer, P., & Junne, S. (2010). Scale-down simulators for metabolic analysis of large-scale bioprocesses. *Current Opinion in Biotechnology*, *21*(1), 114–121. https://doi.org/10.1016/j.copbio.2010.02.001

Nikel, P. I., Fuhrer, T., Chavarría, M., Sánchez-Pascuala, A., Sauer, U., & de Lorenzo, V. (2020). Redox stress reshapes carbon fluxes of *Pseudomonas putida* for cytosolic glucose oxidation and NADPH generation. *bioRxiv*, https://doi.org/10.1101/2020.06.13.149542

Nikel, P. I., & de Lorenzo, V. (2013). Engineering an anaerobic metabolic regime in *Pseudomonas putida* KT2440 for the anoxic biodegradation of 1,3-dichloroprop-1-ene. *Metabolic Engineering*, *15*, 98–112. https://doi.org/10.1016/j.ymben.2012.09.006

Nikel, P. I., & de Lorenzo, V. (2014). Robustness of *Pseudomonas putida* KT2440 as a host for ethanol biosynthesis. *New Biotechnology*, *31*(6), 562–571. https://doi.org/10.1016/j.nbt.2014.02.006

Nikel, P. I., & de Lorenzo, V. (2018). *Pseudomonas putida* as a functional chassis for industrial biocatalysis: From native biochemistry to *trans*-metabolism. *Metabolic Engineering*, *50*, 50142–155. https://doi.org/10.1016/j.ymben.2018.05.005

Nitschel, R., Ankenbauer, A., Welsch, I., Wirth, N. T., Massner, C., Ahmad, N., McColm, S., Borges, F., Fotheringham, I., Takors, R., & Blombach, B. (2020). Engineering *Pseudomonas putida* KT2440 for the production of isobutanol. *Engineering in Life Sciences*, *20*(5–6), 148–159. https://doi.org/10.1002/elsc.201900151

Obruca, S., Sedlacek, P., Koller, M., Kucera, D., & Pernicova, I. (2018). Involvement of polyhydroxyalkanoates in stress resistance of microbial cells: Biotechnological consequences and applications. *Biotechnology Advances*, *36*(3), 856–870. https://doi.org/10.1016/j.biotechadv.2017.12.006

Olughu, W., Deepika, G., Hewitt, C., & Rielly, C. (2019). Insight into the large-scale upstream fermentation environment using scaled-down models. *Journal of Chemical Technology & Biotechnology*, *94*(3), 647–657. https://doi.org/10.1002/jctb.5804

Ramos, J.-L., Sol Cuenca, M., Molina-Santiago, C., Segura, A., Duque, E., Gomez-Garcia, M. R., Udaondo, Z., & Roca, A. (2015). Mechanisms of solvent resistance mediated by interplay of cellular factors in *Pseudomonas putida*. *FEMS Microbiology Reviews*, *39*(4), 555–566. https://doi.org/10.1093/femsre/fuv006

Rodriguez, A., Escobar, S., Gomez, E., Santos, V. E., & Garcia-Ochoa, F. (2018). Behavior of several *Pseudomonas putida* strains growth under different agitation and oxygen supply conditions. *Biotechnology Progress*, *34*(4), 900–909. https://doi.org/10.1002/btpr.2634

Santos, P. M., Benndorf, D., & Sá-Correia, I. (2004). Insights into *Pseudomonas putida* KT2440 response to phenol-induced stress by quantitative proteomics. *Proteomics*, *4*(9), 2640–2652. https://doi.org/10.1002/pmic.200300793

Schmitz, S., Nies, S., Wierckx, N., Blank, L. M., & Rosenbaum, M. A. (2015). Engineering mediator-based electroactivity in the obligate aerobic bacterium *Pseudomonas putida* KT2440. *Frontiers in Microbiology*, *6*, 284. https://doi.org/10.3389/fmicb.2015.00284

Simon, O., Klebensberger, J., Mukschel, B., Klaiber, I., Graf, N., Altenbuchner, J., Huber, A., Hauer, B., & Pfannstiel, J. (2015). Analysis of the molecular response of *Pseudomonas putida* KT2440 to the next-generation biofuel n-butanol. *Journal of Proteomics*, *122*, 11–25. https://doi.org/10.1016/j.jprot.2015.03.022

Sohn, S. B., Kim, T. Y., Park, J. M., & Lee, S. Y. (2010). *In silico* genome-scale metabolic analysis of *Pseudomonas putida* KT2440 for polyhydroxyalkanoate synthesis, degradation of aromatics and anaerobic survival. *Biotechnology Journal*, *5*(7), 739–750. https://doi.org/10.1002/biot.201000124

Soini, J., Ukkonen, K., & Neubauer, P. (2008). High cell density media for *Escherichia coli* are generally designed for aerobic cultivations – Consequences for large-scale bioprocesses and shake flask cultures. *Microbial Cell Factories*, *7*(1):26. https://doi.org/10.1186/1475-2859-7-26

van Sonsbeek, H. M., Beeftink, H. H., & Tramper, J. (1993). Two-liquid-phase bioreactors. *Enzyme and Microbial Technology*, *15*(9), 722–729. https://doi.org/10.1016/0141-0229(93)90001-I

Steen, A., Ütkür, F. Ö., Borrero-de Acuña, J. M., Bunk, B., Roselius, L., Bühler, B., Jahn, D., & Schobert, M. (2013). Construction and characterization of nitrate and nitrite respiring *Pseudomonas putida* KT2440 strains for anoxic biotechnical applications. *Journal of Biotechnology*, *163*(2), 155–165. https://doi.org/10.1016/j.jbiotec.2012.09.015

Tatusov, R. L., Koonin, E. V., & Lipman, D. J. (1997). A genomic perspective on protein families. *Science*, *278*(5338), 631–637. https://doi.org/10.1126/science.278.5338.631

Thompson, M. G., Incha, M. R., Pearson, A. N., Schmidt, M., Sharpless, W. A., Eiben, C. B., Cruz-Morales, P., Blake-Hedges, J. M., Liu, Y., Adams, C. A., Haushalter, R. W., Krishna, R. N., Lichtner, P., Blank, L. M., Mukhopadhyay, A., Deutschbauer, A. M., Shih, P. M., Keasling, J. D., & Zhou, N. Y. (2020). Fatty acid and alcohol metabolism in *Pseudomonas putida*: Functional analysis using random barcode transposon sequencing. *Applied and Environmental*

Microbiology, *86*(21):e01665-20. https://doi.org/10.1128/AEM.01665-20

Timoumi, A., Bideaux, C., Guillouet, S. E., Allouche, Y., Molina-Jouve, C., Fillaudeau, L., & Gorret, N. (2017). Influence of oxygen availability on the metabolism and morphology of *Yarrowia lipolytica*: Insights into the impact of glucose levels on dimorphism. *Applied Microbiology and Biotechnology*, *101*(19), 7317–7333. https://doi.org/10.1007/s00253-017-8446-7

Tiso, T., Ihling, N., Kubicki, S., Biselli, A., Schonhoff, A., Bator, I., Thies, S., Karmainski, T., Kruth, S., Willenbrink, A.-L., Loeschcke, A., Zapp, P., Jupke, A., Jaeger, K.-E., Büchs, J., & Blank, L. M. (2020). Integration of genetic and process engineering for optimized rhamnolipid production using *Pseudomonas putida*. *Frontiers in Bioengineering and Biotechnology*, *8*, 976. https://doi.org/10.3389/fbioe.2020.00976

Tiso, T., Narancic, T., Wei, R., Pollet, E., Beagan, N., Schröder, K., Honak, A., Jiang, M., Kenny, S. T., Wierckx, N., Perrin, R., Avérous, L., Zimmermann, W., O'Connor, K., & Blank, L. M. (2021). Towards bio-upcycling of polyethylene terephthalate. *Metabolic Engineering*, *66*, 167–178. https://doi.org/10.1016/j.ymben.2021.03.011

Tiso, T., Sabelhaus, P., Behrens, B., Wittgens, A., Rosenau, F., Hayen, H., & Blank, L. M. (2016). Creating metabolic demand as an engineering strategy in *Pseudomonas putida* – Rhamnolipid synthesis as an example. *Metabolic Engineering Communications*, *3*, 234–244. https://doi.org/10.1016/j.meteno.2016.08.002

Tiso, T., Wierckx, N., & Blank, L. M. (2014). Non-pathogenic *Pseudomonas* as platform for industrial biocatalysis. In P. Grunwald (Ed.), *Industrial biocatalysis* (Vol. 1). Jenny Stanford Publishing.

Traxler M. F., Zacharia V. M., Marquardt S., Summers S. M., Nguyen H.-T., Stark S. E., Conway T. (2011). Discretely calibrated regulatory loops controlled by ppGpp partition gene induction across the 'feast to famine' gradient in Escherichia coli. *Molecular Microbiology*, *79*(4), 830–845. http://dx.doi.org/10.1111/j.1365-2958.2010.07498.x

Vallon, T., Glemser, M., Malca, S. H., Scheps, D., Schmid, J., Siemann-Herzberg, M., Hauer, B., & Takors, R. (2013). Production of 1-octanol from n-octane by *Pseudomonas putida* KT2440. *Chemie Ingenieur Technik*, *85*(6), 841–848. https://doi.org/10.1002/cite.201200178

Vallon, T., Simon, O., Rendgen-Heugle, B., Frana, S., Mückschel, B., Broicher, A., Siemann-Herzberg, M., Pfannenstiel, J., Hauer, B., Huber, A., Breuer, M., & Takors, R. (2015). Applying systems biology tools to study n-butanol degradation in *Pseudomonas putida* KT2440. *Engineering in Life Sciences*, *15*(8), 760–771. https://doi.org/10.1002/elsc.201400051

Voges, R., & Noack, S. (2012). Quantification of proteome dynamics in *Corynebacterium glutamicum* by (15)N-labeling and selected reaction monitoring. *Journal of Proteomics*, *75*(9), 2660–2669. https://doi.org/10.1016/j.jprot.2012.03.020

Weber, B., Campenhausen, M., von, Maßmann, T., Bednarz, A., & Jupke, A. (2019). CFD based compartment-model for a multiphase loop-reactor. *Chemical Engineering Science: X*, *2*, 100010. https://doi.org/10.1016/j.cesx.2019.100010

Wehrmann, M., Elsayed, E. M., Köbbing, S., Bendz, L., Lepak, A., Schwabe, J., Wierckx, N., Bange, G., & Klebensberger, J. (2020). Engineered PQQ-dependent alcohol dehydrogenase for the oxidation of 5-(hydroxymethyl)furoic acid. *ACS Catalysis*, *10*(14), 7836–7842. https://doi.org/10.1021/acscatal.0c01789

Weimer, A., Kohlstedt, M., Volke, D. C., Nikel, P. I., & Wittmann, C. (2020). Industrial biotechnology of *Pseudomonas putida*: Advances and prospects. *Applied Microbiology and Biotechnology*, *104*(18), 7745–7766. https://doi.org/10.1007/s00253-020-10811-9

Wierckx, N. J. P., Ballerstedt, H., Bont, J. A. M., & de, Wery, J. (2005). Engineering of solvent-tolerant *Pseudomonas putida* S12 for bioproduction of phenol from glucose. *Applied and Environmental Microbiology*, *71*(12), 8221–8227. https://doi.org/10.1128/AEM.71.12.8221-8227.2005

Yu, S., Lai, B., Plan, M. R., Hodson, M. P., Lestari, E. A., Song, H., & Krömer, J. O. (2018). Improved performance of *Pseudomonas putida* in a bioelectrochemical system through overexpression of periplasmic glucose dehydrogenase. *Biotechnology and Bioengineering*, *115*(1), 145–155. https://doi.org/10.1002/bit.26433

SUPPORTING INFORMATION

Additional Supporting Information may be found online in the supporting information tab for this article.

How to cite this article: Demling, P., Ankenbauer, A., Klein, B., Noack, S., Tiso, T., Takors, R., & Blank, L. M. (2021). *Pseudomonas putida* KT2440 endures temporary oxygen limitations. *Biotechnology and Bioengineering*, 118, 4735–4750. https://doi.org/10.1002/bit.27938